

Direct photon emission from hadronic sources: Hydrodynamics vs. Transport theory

Bjørn Bäuchle^{1,2} and Marcus Bleicher²

¹ Frankfurt Institute for Advanced Studies, Ruth-Moufang-Str. 1, 60438 Frankfurt am Main

² Institut für Theoretische Physik, Johann Wolfgang Goethe-Universität, Max-von-Laue-Str. 1, 60438 Frankfurt am Main, Germany

Received: date / Revised version: date

Abstract. Direct photon emission in heavy-ion collisions is calculated within the relativistic microscopic transport model UrQMD. We compare the results from the pure transport calculation to a hybrid-model calculation, where the high-density part of the evolution is replaced by an ideal 3-dimensional fluiddynamic calculation. The effects of viscosity, present in the transport model but neglected in ideal fluid-dynamics, are examined. We study the contribution of different production channels and non-thermal collisions to the spectrum of direct photons. Detailed comparison to the measurements by the WA 98-collaboration are undertaken.

PACS. XX.XX.XX No PACS code given

1 Introduction

The creation and study of high-density and -temperature nuclear matter is the major goal of heavy-ion experiments. If the energy density in the reaction is high enough, a state of quasi-free partonic degrees of freedom, a Quark-Gluon-Plasma (QGP) [1,2], may be formed. Recent experimental observations at the Relativistic Heavy Ion Collider (BNL-RHIC) like e.g. strong jet quenching and high elliptic flow

hint to the creation of a strongly coupled QGP (sQGP) [3, 4,5,6]. Possible evidence for the creation of this new state of matter has also been put forward by collaborations at the Super Proton Synchrotron (CERN-SPS), as for instance the step in the mean transverse mass excitation function of protons, kaons and pions and the enhanced K^+/π^+ -ratio [7].

Unfortunately, it is not yet possible to describe the time evolution of the produced matter from first principle

Quantum Chromodynamics (QCD). Neither can the hot part of a collision be observed directly. Therefore well-developed dynamical models to describe the space-time evolution of nuclear interactions are needed. Among those approaches is relativistic transport theory [8,9,10,11,12,13]. In this kind of microscopic description, the hadronic and/or the partonic stage of the collision can be described under certain approximations. E.g. most transport models cannot describe collisions with more than two incoming particles restricting the applicability to low particle densities, where multi-particle interactions are less important. Some attempts to include multi-particle interactions do exist [14,11,15,16,17], but this field of study is still rather new. The coupling of a partonic phase with a hadronic phase imposes one more problem on transport models. The microscopic details of that transition are not known. There are several attempts to address the problem of microscopic hadronization [12,18,19,20,21,22]. One caveat in transport approach is that all microscopic scatterings are explicitly in the model and therefore the cross-sections for all processes must be known or extrapolated. However, for most processes no experimental data are available, and a large fraction of cross-sections have to be calculated or parametrized by additional models.

Relativistic, non-viscous, perfect fluid-dynamics is a different approach to explore the space-time evolution of a heavy-ion collision. It constitutes a macroscopic description of the matter that is created, assuming that at every time and in every place it is in perfect local thermal equilibrium. This assumption can only be true if the matter

is sufficiently dense, so in the late stages of a heavy-ion collision fluid-dynamics loses applicability. An advantage is that in the dense stages, hydrodynamics can propagate any kind of matter, and also allows for transitions between two types of matter, e.g. QGP and hadron gas, if an appropriate Equation of State (EoS) is provided. Fluid-dynamics can therefore be used to study hadronic and partonic matter in one common model.

The restrictions of this kind of model can be loosened as well. By introducing viscosity and heat conductivity, perfect thermal equilibrium does not have to be present at any point. However, even with second order corrections the matter has to be close to equilibrium.

Input to solve the hydrodynamic differential equations are the boundaries, i.e. the initial state (the distributions of all relevant densities and currents at the time the evolution starts), the Equation of State providing the pressure as function of the energy and baryon densities, that describes the behaviour of the matter that is considered, and the freeze-out hypersurface.

Out of the many possible observables, electromagnetic probes have the advantage of leaving undisturbed: once they are created, they will escape the reaction zone, due to negligible rescattering cross-sections. Besides dileptons, direct photon emission is therefore of greatest interest to gain insight into the early, hot and therefore possibly partonic stages of a reaction. Direct photons are distinguished from the mass of photons as those coming from collisions and not decays.

Unfortunately, most photons in heavy-ion collisions come from hadronic decays in the very late stages, mostly $\pi^0 \rightarrow \gamma\gamma$. These decay-photons impose a serious challenge to the experimentalists when they try to obtain the spectra of direct photons. Up to now, several experiments have tried to obtain the spectra of direct photons: Helios, WA 80 and CERES (all at CERN-SPS) could publish upper limits, while WA 98 (CERN-SPS) and PHENIX (BNL-RHIC) have published data points for direct photons.

Approaches to the theoretical description of direct photon spectra include calculations with perturbative Quantum-Chromo-Dynamics (pQCD), the application of thermal rates and microscopic cross-sections, all of which have their area of applicability.

Calculations based on pQCD describe the photon data in proton-proton collisions very well and, if scaled by the number of binary collisions, also those in heavy-ion reactions. The range of applicability is limited to high transverse momentum $p_{\perp}^{\gamma} \gg 1$ GeV.

Thermal rates can only be applied if the assumption of local thermal equilibrium is fulfilled. Scattering rates can then be calculated by folding the particle distribution functions of the participating particle species with the respective cross-sections. This framework can be applied to either static models, simplified hydrodynamics-inspired models such as the blast wave model and to full fluid-dynamic calculations. The space-time evolution of a reaction as predicted by microscopic theories can be av-

eraged over in order to apply thermal rates to the coarse-grained distributions [23].

The application of microscopic cross-sections can only be undertaken in a model where all microscopic collisions are known. That limits the field of use to transport models. There have been several calculations for photon spectra from transport models [24,25]

In this paper we first introduce the dynamic models used for the calculations. Then, we explain the cross-sections and thermal rates used for photon emission as well as the mechanisms for doing so. Following that, the results of our calculations are presented and compared to results from the WA 98-collaboration. Finally, after summary and conclusions, an outlook to further planned studies is given.

2 UrQMD hybrid model

UrQMD (Ultra-relativistic Quantum Molecular Dynamics) is a microscopic transport model. It includes all hadrons and resonances up to masses $m = 2.2$ GeV and at high energies can excite and fragment strings. The cross-sections are either calculated via detailed balance or parametrized by the additive quark model (AQM), if no experimental values are available. At high parton momentum transfers, PYTHIA is employed for pQCD scatterings. UrQMD has been used by Dumitru *et al* to study direct photon emission earlier [24].

In this work, we combine and compare the two models mentioned above to describe the space-time evolution of a heavy-ion reaction: for the unequilibrated initial state and the low-density final state, the microscopic transport

model UrQMD is used, whereas the high-density part of the reaction is modelled using ideal 3+1-dimensional fluid-dynamics. For details of this model see [26]. During the evolution, two mappings have to be performed: After the incoming nuclei have passed each other, the baryon-number-, energy- and momentum-densities are smoothed and put into the hydro calculation. After the local rest frame energy density has dropped below a threshold value of $\epsilon_{\text{crit}} = 730 \text{ MeV/fm}^3 (\approx 5\epsilon_0)$ in every point, particles are created from the densities by means of the Cooper-Frye formula and propagation is continued in UrQMD. The effect of changing those parameters is studied in [26] and found to be small.

For the present studies, the EoS used in the hydrodynamic part resembles a free hadron gas with the same degrees of freedom that the transport part (i.e., UrQMD) has. Since strings are expected to be created in scatterings with very high center-of-mass energies, and since hydrodynamics only describes soft scatterings, they are not included in the EoS.

By this choice, one can study the impact of different underlying dynamics of the reaction on the spectra of photons. This allows to disentangle which changes are due to different physical assumptions. In further work, we plan to explore to the EoS, i.e, changes to the assumptions of the underlying medium (chirally restored or deconfined matter).

3 Photon emission from hadronic sources

In both models, hybrid and pure transport, photon emission is calculated perturbatively. That means, the evolution of the underlying event is not changed by the emission of photons. This is justified as the emission probability for photons is extremely small.

3.1 Photons from UrQMD

In the transport part of our calculations for each scattering the cross-section for photon production is calculated. Cross-sections are taken from Kapusta *et al* [27] and Xiong *et al* [28]. In the former work, the photon self-energy from a Lagrangian involving the pion, rho and photon-fields has been taken as basis for the calculations:

$$\mathcal{L} = |D_\mu \Phi|^2 - m_\pi^2 |\Phi|^2 - \frac{1}{4} \rho_{\mu\nu} \rho^{\mu\nu} + \frac{1}{2} m_\rho^2 \rho_\mu \rho^\mu - \frac{1}{4} F_{\mu\nu} F^{\mu\nu} \quad (1)$$

(for details the reader is referred to [27]). The coupling of the ρ - to the π -meson is characterized by the coupling constant g_ρ , which is inferred from the decay rate $\rho \rightarrow \pi\pi$ with $g_\rho^2/4\pi = 12\Gamma\omega_0^3/(m_\rho p_0^3)$. Here, p_0 and ω_0 are the momentum and energy of a decay- π in the rest frame of the ρ and Γ is the decay-width. Kapusta *et al* argue that Γ is experimentally measured and therefore effectively includes certain higher-order effects such as vertex corrections.

From this Lagrangian, they calculate cross-sections for the following processes:

$$\begin{aligned} \pi^\pm \pi^\mp &\rightarrow \gamma \rho^0, \\ \pi^\pm \pi^0 &\rightarrow \gamma \rho^\pm, \end{aligned}$$

$$\begin{aligned}\pi^\pm \rho^0 &\rightarrow \gamma \pi^\pm, \\ \pi^\pm \rho^\mp &\rightarrow \gamma \pi^0, \\ \pi^0 \rho^\pm &\rightarrow \gamma \pi^\pm, \\ \pi^\pm \pi^\mp &\rightarrow \gamma \gamma.\end{aligned}$$

The last of these is suppressed by an additional factor of α with respect to the others and is therefore not expected to contribute to the photon spectra significantly.

Kapusta *et al* also quote cross-sections involving the η -meson ($\pi^\pm \pi^\mp \rightarrow \gamma \eta$ and $\pi^\pm \eta \rightarrow \gamma \pi^\pm$), but they are omitted in our calculations.

From the paper by Xiong *et al*, we deduce the cross-sections for the processes

$$\pi \rho \rightarrow a_1 \rightarrow \gamma \pi,$$

averaged over all possible charge combinations. This channel is not included in Kapusta *et al*.

In order to obtain photon spectra, all scatterings that happen during the transport phase are examined. For every scattering that can produce photons, the corresponding fraction of a photon

$$N_\gamma^t = \frac{\sigma_{\text{em}}}{\sigma_{\text{tot}}} \quad (2)$$

is produced. In this formula, σ_{tot} is the sum of the total hadronic cross-section for a collision with these ingoing particles (known from UrQMD) and the electromagnetic cross-section σ_{em} as calculated by the formulæ from the abovementioned papers.

This number of photons N_γ^t is then distributed in the solid angle by the angular distributions as given by $d\sigma/dt$, so that a whole distribution of fractional photons per colli-

sion instead of only one (complete) photon every $\sim 10,000$ collisions is created. This allows us to have a much better statistics with less hadronic events. The small cross-sections for the processes we consider justify this perturbative ansatz.

3.2 Photons from hydrodynamics

For the hydro-evolution we also produce fractional photons at every cell of the hydrodynamic calculation. We use the parametrizations by Turbide, Rapp and Gale [29].

To obtain these, they start with an effective non-linear σ -model Lagrangian with the vector and axial vector fields implemented as massive gauge fields of the chiral $U(3)_L \times U(3)_R$ symmetry. They calculate a different set of rates than cross-sections calculated by Kapusta *et al*, namely:

$$\pi \pi \rightarrow \gamma \rho,$$

$$\pi \rho \rightarrow \gamma \pi,$$

$$\pi K^* \rightarrow \gamma K,$$

$$\pi K \rightarrow \gamma K^*,$$

$$\rho K \rightarrow \gamma K,$$

$$K^* K \rightarrow \gamma \pi.$$

The rate for $\pi \rho \rightarrow \gamma \pi$ contains the process $\pi \rho \rightarrow a_1 \rightarrow \gamma \pi$.

The rates involving K and K^* are included in our calculation albeit they are negligible compared to the others.

Turbide *et al* also calculate the emission rate from ρ -decay ($\rho \rightarrow \pi \pi \gamma$), but this is not taken into account for the present work, because we want to restrict ourselves to collisional photons.

For every cell, we generate one fractional photon, its fraction being the integral over the invariant rate:

$$N_\gamma^h = \Delta V \Delta t \int \frac{d^3 p}{E} E \frac{dR}{d^3 p}, \quad (3)$$

where ΔV and Δt are cell volume and time step, respectively, and $E dR/d^3 p$ is the rate for photon emission as given by Turbide *et al.*

To get photon spectra with the right lab-frame distribution out of the (spherically symmetric) local-rest-frame distribution, a lorentz-transformation has to be applied to the generated photons.

We choose the invariant generalization of the energy $p_\mu u^\mu$ according to the distribution functions implied by the rates. Then we choose a p^μ which, together with the cell's flow velocity u^μ , results in the desired $p_\mu u^\mu$.

One fractional photon is then created in the direction of this p^μ with the fraction N_γ^h .

4 Results

All calculations are done for Pb+Pb-collisions at incident beam energy of $E_{\text{Lab}} = 158 \text{ AGeV}$. The sample of collisions has impact parameters of $b \leq 4.5 \text{ fm}$ and only midrapidity-photons ($|y_{\text{c.m.}}| < 0.5$) are included in the analysis. These settings are equivalent to the WA 98 trigger conditions and detector setups for their ‘‘central’’ data set [30,31].

4.1 Emission times

Due to formation time effects and the Heisenberg principle, particles cannot be produced earlier than $t_{\text{prod}} \approx E^{-1}$.

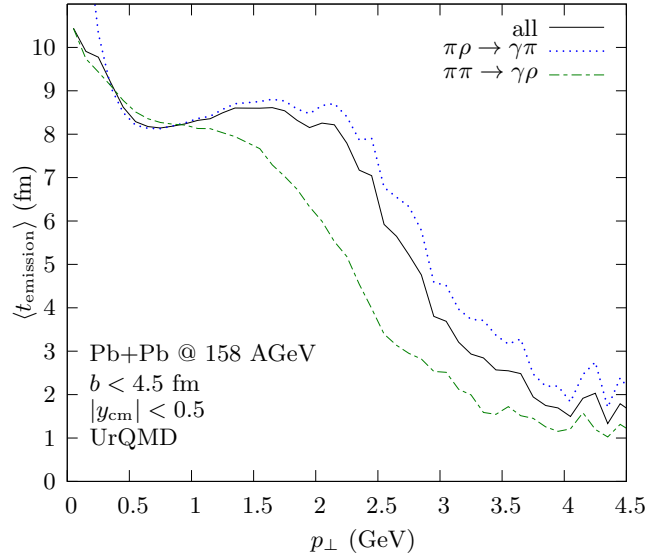


Fig. 1. (Color Online.) Average emission time of direct photons vs. transverse momentum. The curve for $\pi\pi \rightarrow \gamma\gamma$ is omitted from the plot; the emission times for that rate are much higher than the range of the plot.

For photons at mid-rapidity, where $E = p_\perp$, this gives a lower bound for particle production times in different p_\perp -bins.

Later emission times, though, are well possible. If a particular scattering occurs preferably at late times, the average emission time of photons may be shifted to later times.

In this analysis only scatterings between mesons are considered as photon sources. Mesons have to be produced in a heavy ion collision, so it can be assumed that meson-meson scatterings occur only after some time.

Figure 1 shows the average emission times of all photons as well as of those photons coming from $\pi\rho$ - and $\pi\pi$ -scatterings. The complete average is obviously dominated by the processes with π and ρ in the initial state, as is consistent with the results in section 4.2.

It is eye-catching that the average emission times of the photons deviate a lot from the hyperbolic behaviour mentioned earlier. Especially in the intermediate p_{\perp} -region of 1 – 2.5 GeV it becomes apparent that photons are produced from decay products that have not been present in the collision before 5 or 6 fm. $\pi\pi$ -scatterings contribute at the same times, but at lower momenta ($p_{\perp} \approx 0.5 - 1.5$ GeV).

4.2 Photon spectra

Figure 2 (left) shows the direct photon spectra from a pure transport calculation. The most dominant contribution to the spectra is the channel $\pi\rho \rightarrow \gamma\pi$, which contributes about on order of magnitude more than the sum over all other channels between $p_{\perp} = 0.5$ GeV and $p_{\perp} = 2.5$ GeV.

Emission from all channels is very thermalized at low transverse momenta, and the $\pi\pi \rightarrow \gamma\rho$ - and $\pi\rho \rightarrow \gamma\pi$ -channels contribute significantly at high p_{\perp} , where pre-equilibrium scatterings play an important role.

As expected, the doubly-electromagnetic channel $\pi\pi \rightarrow \gamma\gamma$ is very much suppressed over the whole p_{\perp} -range.

The relative contributions of the different channel are very similar in the case of a hybrid-model calculation. Figure 2 (right) shows the spectra obtained in that case. Here, the dominance of the $\pi\rho$ -channel is as pronounced as in the pure transport calculation. Overall, contributions from that channel and the $\pi\pi$ -channel look rather similar to the UrQMD-case above a momentum of about $p_{\perp} \approx 1$ GeV, because in this regime the non-equilibrium phases contribute more than the high-density hydro phase.

In UrQMD, the leading particles from a string have a reduced cross-section during their formation time. The effects of neglecting photons coming from collisions of string ends is shown in Figure 2. The difference becomes important at high p_{\perp} , where photons from initial hard pQCD-scatterings play an important role.

For comparison, we show the pQCD-spectrum in Figure 2 (taken from [33]) where an intrinsic $\langle k_{\perp}^2 \rangle \approx 0.9$ GeV² was used. One clearly observes that pQCD photons are a dominant source of photons at high p_{\perp} , especially if the (slightly artificial) contribution from string ends is removed from the spectrum.

For a comparison between hybrid- and transport-calculation we restrict the analysis to those channels that are present in both models. Figure 3 shows spectra for $\pi\pi \rightarrow \gamma\rho$ plus $\pi\rho \rightarrow \gamma\pi$ for pure transport and the complete hybrid model. The different stages to the hybrid model (pre-equilibrium, hydro, post-freeze-out) are separately plotted.

The yield at low $p_{\perp} < 1$ GeV is dominated by radiation from the hydro phase. Above that value, most photons come from the post-freeze-out and pre-equilibrium stages. It is interesting to see that the photon yield in the range 1 GeV $< p_{\perp} < 2.5$ GeV is dominated by photons coming from post-freeze-out scatterings. This is consistent with the observation of late emission times in that p_{\perp} -range as shown in Figure 1.

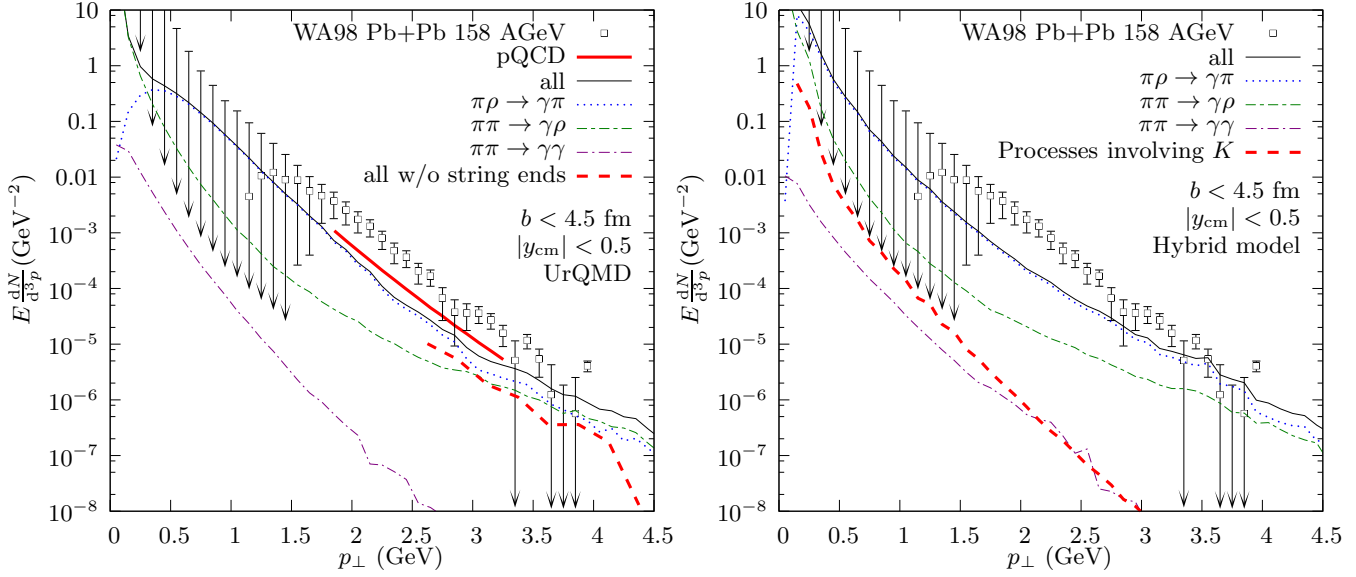


Fig. 2. (Color Online.) Transverse momentum spectra of direct photons from both models. Left: pure UrQMD, right: Hybrid. The different charge combinations of the channels have been combined for better clarity. Experimental data taken from [30] (“central” data set, table IV), arrows indicate b data points where the error band extends to negative yields. In the left figure, a pQCD-spectrum from the initial proton-proton-collisions [32,33] is shown, as well as the spectrum from pure UrQMD when neglecting the contribution from string ends (see text).

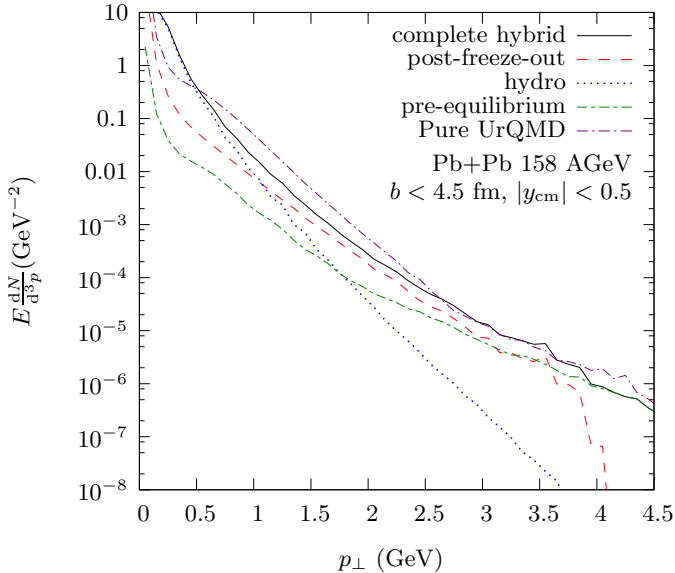


Fig. 3. (Color Online.) Transverse momentum spectra of direct photons compared between both approaches.

5 Summary

In this work, we have shown the direct photon spectra for central Pb+Pb-collisions at top SPS energies. We have

used and compared two different models, both of which give similar results. UrQMD, as a purely hadronic transport model, underpredicts the data from WA 98 below $p_{\perp} = 3.5$ GeV. The hybrid calculation, where the high-density phase of the evolution is described by hydrodynamics, also underpredicts the data in that range.

In both cases, processes with π and ρ in the initial state dominate the intermediate and low momentum regions and processes with two π become important at high momenta, where early scatterings dominate.

Emission times for direct photons at intermediate transverse momenta are found to be very late, and so this p_{\perp} -range is in the hybrid model dominated by photons from the late post-freeze-out stage.

At very low p_{\perp} , the hydro phase contributes much more to the photon spectra than the transport phase does. Here, the only significant difference between both models is seen.

6 Conclusions

The hadronic models used in the current work cannot reproduce the direct photon spectra as measured by WA 98. The reason for this remains unclear; it could be that the implementation of more channels is necessary. It is also possible that using an EoS with phase-transition to a QGP will yield significantly higher spectra. The addition of photons from hard pQCD-scatterings will contribute significantly, though not sufficiently, to the final spectrum. Most probably, each of these points will contribute to the missing photons.

7 Outlook

The work presented here lays the foundation for many further investigations. First, photons from initial hard pQCD-scatterings have to be added. Other collisions with high \sqrt{s} have to be treated with pQCD instead of hadronic cross-sections as well. The channels that are implemented in both stages of the model (transport and hydrodynamics) have to be aligned, so that a comparison does not have to be confined to the smallest common denominator. Also, the list of channels in both cases has to be extended beyond what is implemented so far. Scatterings involving

the η -meson as well as baryonic processes should be among those that are added next.

Also, the existing channels can be improved: Until now, the channels that involve a ρ -meson as outgoing particle always assume that the ρ -meson is produced at its pole mass, which clearly does not have to be the case.

On the part of the hydro evolution, it is of course of great interest to study the emission of direct photons from thermal partonic processes, i.e. the inclusion of an EoS containing a phase transition to a QGP is necessary. Comparisons to data from RHIC and predictions for the new FAIR-facility will be accessible then.

8 Acknowledgements

This work has been supported by the Frankfurt Center for Scientific Computing (CSC), the GSI and the BMBF. The authors thank Hannah Petersen for providing the hybrid- and Dirk Rischke for the hydro-code. B. Bäuchle gratefully acknowledges support from the Deutsche Telekom Stiftung and the Helmholtz Research School on Quark Matter Studies. This work was partially supported by the Hessian LOEWE initiative Helmholtz International Center for FAIR.

References

1. J. W. Harris and B. Muller, *Ann. Rev. Nucl. Part. Sci.* **46** (1996) 71 [arXiv:hep-ph/9602235].
2. S. A. Bass, M. Gyulassy, H. Stoecker and W. Greiner, *J. Phys. G* **25** (1999) R1 [arXiv:hep-ph/9810281].

3. J. Adams *et al.* [STAR Collaboration], Nucl. Phys. A **757** (2005) 102 [arXiv:nucl-ex/0501009].
4. B. B. Back *et al.*, Nucl. Phys. A **757** (2005) 28 [arXiv:nucl-ex/0410022].
5. I. Arsene *et al.* [BRAHMS Collaboration], Nucl. Phys. A **757** (2005) 1 [arXiv:nucl-ex/0410020].
6. K. Adcox *et al.* [PHENIX Collaboration], Nucl. Phys. A **757** (2005) 184 [arXiv:nucl-ex/0410003].
7. C. Alt *et al.* [NA49 Collaboration], Phys. Rev. C **77** (2008) 024903 [arXiv:0710.0118 [nucl-ex]].
8. S. A. Bass *et al.*, Prog. Part. Nucl. Phys. **41** (1998) 255 [Prog. Part. Nucl. Phys. **41** (1998) 225] [arXiv:nucl-th/9803035].
9. M. Bleicher *et al.*, J. Phys. G **25** (1999) 1859 [arXiv:hep-ph/9909407].
10. D. Molnar and P. Huovinen, Phys. Rev. Lett. **94** (2005) 012302 [arXiv:nucl-th/0404065].
11. Z. Xu and C. Greiner, Phys. Rev. C **71** (2005) 064901 [arXiv:hep-ph/0406278].
12. Z. W. Lin, C. M. Ko, B. A. Li, B. Zhang and S. Pal, Phys. Rev. C **72** (2005) 064901 [arXiv:nucl-th/0411110].
13. G. Baur, J. Bleibel, C. Fuchs, A. Faessler, L. V. Bravina and E. E. Zabrodin, Phys. Rev. C **71** (2005) 054905 [arXiv:nucl-th/0411117].
14. H. W. Barz and B. Kampfer, Nucl. Phys. A **683** (2001) 594 [arXiv:nucl-th/0005063].
15. A. B. Larionov, O. Buss, K. Gallmeister and U. Mosel, Phys. Rev. C **76** (2007) 044909 [arXiv:0704.1785 [nucl-th]].
16. J. Bleibel, G. Baur, A. Faessler and C. Fuchs, Phys. Rev. C **76** (2007) 024912 [arXiv:nucl-th/0610021].
17. J. Bleibel, G. Baur and C. Fuchs, Phys. Lett. B **659** (2008) 520 [arXiv:0711.3366 [nucl-th]].
18. B. Andersson, G. Gustafson and C. Peterson, Nucl. Phys. B **135** (1978) 273.
19. J. R. Ellis and K. Geiger, Phys. Rev. D **52** (1995) 1500 [arXiv:hep-ph/9503349].
20. C. T. Traxler, U. Mosel and T. S. Biro, Phys. Rev. C **59** (1999) 1620 [arXiv:hep-ph/9808298].
21. T. S. Biro, P. Levai and J. Zimanyi, Phys. Rev. C **59** (1999) 1574 [arXiv:hep-ph/9807303].
22. M. Hofmann, M. Bleicher, S. Scherer, L. Neise, H. Stoecker and W. Greiner, Phys. Lett. B **478** (2000) 161 [arXiv:nucl-th/9908030].
23. P. Huovinen, M. Belkacem, P. J. Ellis and J. I. Kapusta, Phys. Rev. C **66** (2002) 014903 [arXiv:nucl-th/0203023].
24. A. Dumitru, M. Bleicher, S. A. Bass, C. Spieles, L. Neise, H. Stoecker and W. Greiner, Phys. Rev. C **57** (1998) 3271 [arXiv:hep-ph/9709487].
25. E. L. Bratkovskaya, S. M. Kiselev and G. B. Sharkov, Phys. Rev. C **78** (2008) 034905 [arXiv:0806.3465 [nucl-th]].
26. H. Petersen, J. Steinheimer, G. Baur, M. Bleicher and H. Stoecker, Phys. Rev. C **78** (2008) 044901 [arXiv:0806.1695 [nucl-th]].
27. J. I. Kapusta, P. Lichard and D. Seibert, Phys. Rev. D **44** (1991) 2774 [Erratum-ibid. D **47** (1993) 4171].
28. L. Xiong, E. V. Shuryak and G. E. Brown, Phys. Rev. D **46** (1992) 3798 [arXiv:hep-ph/9208206].
29. S. Turbide, R. Rapp and C. Gale, Phys. Rev. C **69** (2004) 014903 [arXiv:hep-ph/0308085].
30. M. M. Aggarwal *et al.* [WA98 Collaboration], arXiv:nucl-ex/0006007.
31. M. M. Aggarwal *et al.* [WA98 Collaboration], Phys. Rev. Lett. **85** (2000) 3595 [arXiv:nucl-ex/0006008].

32. C. Y. Wong and H. Wang, Phys. Rev. C **58** (1998) 376
[arXiv:hep-ph/9802378].
33. C. Gale, Nucl. Phys. A **698** (2002) 143 [arXiv:hep-ph/0104235].